ELSEVIER

Polymer 40 (1999) 2521–2536

polymer

Evolution of a dispersed morphology from a co-continuous morphology in immiscible polymer blends

Je Kyun Lee, Chang Dae Han*

Department of Polymer Engineering, The University of Akron, Akron, OH 44325, USA

Received 7 July 1997; revised 1 May 1998; accepted 23 June 1998

Abstract

We observed, via transmission electron microscopy, the evolution of a dispersed morphology from a modulated co-continuous morphology in immiscible blends of two amorphous polymers, poly(methyl methacrylate) (PMMA) and polystyrene (PS). Upon rapid precipitation of a homogeneous solution, which can be regarded as being equivalent to spinodal decomposition via temperature quenching, we observed a modulated co-continuous morphology for all three blend compositions, 70/30, 50/50, and 30/70 PMMA/PS blends. This observation is interpreted with the Cahn's linearized theory, which has been found to be accurate in describing phase separation in the early stage of spinodal decomposition. When a rapidly precipitated PMMA/PS blend specimen having asymmetric (70/30, 60/40, 55/45 or 30/70) blend composition was annealed under isothermal conditions at 170°C for varying periods, the modulated co-continuous morphology evolved into a dispersed morphology, in which the major component formed the continuous phase and the minor component formed the discrete phase, and into a 'dual mode' of dispersed morphology in the symmetric (50/50) PMMA/PS blend. This observation is interpreted in terms of the percolation-to-cluster transition mechanism proposed by Hashimoto and co-workers. The morphology evolution, during isothermal annealing, of a rapidly precipitated blend may be regarded as being equivalent to late stages of spinodal decomposition, which is controlled by diffusion and coalescence. The rate of morphology development in PMMA/PS blend during isothermal annealing was found to depend on the zero-shear viscosity ratio of the constituent components. This observation is interpreted in terms of Siggia's theory for late stages of spinodal decomposition.

Keywords: Blend morphology; Polymer blends; Rapid precipitation

1. Introduction

In the 1970s Han et al. [1–3], Nelson et al. [4], and van Oene [5] conducted pioneering experimental investigations on morphology–rheology-processing relationships in two-phase polymer blends, and they are summarized in two monographs by Han [6,7]. Although many more experimental studies were reported on the subject since the publication of these two monographs, the fundamental experimental observations reported therein remain the same. Namely, when melt blending two immiscible homopolymers or random copolymers in a mixing equipment, one encounters two types of blend morphology: (i) dispersed morphology and (ii) co-continuous morphology. It has generally been observed [1–7] that a dispersed morphology is formed when the blend composition is highly asymmetric and a co-continuous morphology is formed when the blend composition is symmetric or close to symmetric, and that when a dispersed blend morphology is formed the minor component having higher melt viscosity forms the discrete phase (i.e. droplets) and the major component having lower melt viscosity forms the continuous phase (i.e. matrix).

During the past several years some effort [8–17] has been spent on investigating morphology evolution during melt blending in either a batch mixing equipment (e.g. Brabender mixer) or a continuous mixing equipment (e.g. a twin-screw extruder). Investigators reported the observation of a co-continuous morphology and/or a dispersed morphology, depending upon melt blending conditions and blend compositions. An inversion of the state of dispersion was also reported as the blend ratio varied. At present, however, it is not clear from the literature whether a co-continuous morphology is stable or it is unstable and eventually transforms into a stable, dispersed morphology.

Very recently, using two amorphous polymers, poly(methyl methacrylate) (PMMA) and polystyrene (PS), we carried out an experimental investigation to find out whether or not a co-continuous morphology is stable. For the study

* Corresponding author. Tel.: +1-330-972-6468; Fax: +1-330-972-5720.

0032-3861/99/$ - see front matter
PII: S0032-3861(98)00496-0

we prepared PMMA/PS binary blends using rapid precipitation of a homogeneous solution of PMMA and PS into a non-solvent. We observed a modulated co-continuous morphology, regardless of blend ratio, similar to one usually observed from 'spinodal decomposition' via temperature quenching. When a rapidly precipitated PMMA/PS blend specimen having asymmetric (70/30, 60/40, 55/45 or 30/70) blend composition was annealed under isothermal conditions at 170°C for varying periods, the modulated co-continuous morphology evolved into a dispersed morphology, in which the major component formed the continuous phase and the minor component formed the discrete phase, and into a 'dual mode' of dispersed morphology in the symmetric (50/50) PMMA/PS blend. In this paper we first present our experimental results and then interpret them using currently held theories of spinodal decomposition.

2. Experimental

2.1. Materials

We used the following materials: (1) two monodisperse PSs synthesized via anionic polymerization in our laboratory, (2) a commercial grade of PS (STYRON 615PR, Dow Chemical Company), (3) a laboratory grade of PMMA, and (4) a commercial grade of PMMA (Plexiglas V825, Rohm and Haas Company). Sample codes and the molecular characteristics of the polymers investigated are summarized in Table 1, in which the molecular weight was determined relative to polystyrene standards by gel permeation chromatography. In preparing blends, we used the following three pairs: (1) PMMA-1/PS-1 pair, (2) PMMA-2/PS-2 pair, and (3) PMMA-2/PS-3 pair. These pairs were selected, such that a large variation in zero-shear viscosity ratio of the constituent components could be obtained. Table 2 and Table 3 give sample codes of the three blend systems selected and the zero-shear viscosity ratios of the constituent components at 170°C at which the rapidly precipitated blend specimens were subsequently annealed. For each polymer pair, five blend ratios (by volume) were chosen: 70/30, 60/40, 55/45, 50/50, and 30/70 PMMA/PS.

Table 1
Molecular characteristics of the polymers employed in this study

Sample code	M_w	M_w/M_n
PMMA-1[a]	7.9×10^4	1.56
PMMA-2[b]	4.1×10^4	2.20
PS-1[c]	2.1×10^5	2.00
PS-2[b]	1.1×10^5	1.09
PS-3[b]	3.2×10^5	1.17

[a] Plexiglas V815 (Rohm and Haas).
[b] Laboratory grade.
[c] STYRON 615PR (Dow Chemical).

Table 2
Zero-shear viscosity (η_o) at 170°C of PMMA and PS employed in this study

Sample code	η_o at 170°C (Pa s)
PMMA-1	1.71×10^7
PMMA-2	1.30×10^5
PS-1	6.01×10^4
PS-2	1.15×10^4
PS-3	4.38×10^5

2.2. Rheological measurement

A Rheometrics mechanical spectrometer (RMS Model 800) with a cone-and-plate (25 mm diameter plate, 0.1 radian cone angle) fixture was used to measure steady-state shear viscosity (η) at low shear rates ($\dot{\gamma}$) ranging from 0.001 to ca. 10 s^{-1} and at temperatures ranging from 160 to 240°C. All experiments were conducted under a nitrogen atmosphere in order to preclude oxidative degradation of the specimen. The temperature control was satisfactory to within ±1°C. An Instron capillary rheometer (Mode 3211, Instron Company) with a capillary diameter of 0.15 cm and a length-to-diameter ratio of 28.5 was used to measure the viscosities of the same homopolymers at high shear rates ranging from ca. 10 to 1000 s^{-1}. In calculating shear viscosity, end-corrections were neglected.

2.3. Rapid precipitation

In preparing binary blends of PMMA and PS by rapid precipitation, the two polymers were dissolved in toluene at room temperature to form a homogeneous solution (2 wt% polymer), which was stirred for at least 24 h. Then, the solution was slowly poured into the rapid precipitation setup, which was comprised of a six-blade turbine centrally placed in a perforated draft tube [18,19]. The rapid precipitation setup was maintained at room temperature and the tall form beaker containing both the draft tube and the rotating shaft was charged with methanol. Immediate precipitation of the polymers was observed upon the polymer solution's contact with the circulating methanol pool. The suspension of the precipitated polymers in a liquid mixture of toluene and methanol was filtered at room temperature. After filtration, the precipitated polymers were washed several times to remove toluene by methanol. The washed precipitates were dried at room temperature in a fume hood for one day and then in a vacuum oven at 40°C for one week to

Table 3
Zero-shear viscosity ratio ($\eta_{o,PMMA}/\eta_{o,PS}$) at 170°C of PMMA and PS employed in this study

Sample code	$\eta_{o,PMMA}/\eta_{o,PS}$ at 170°C
PMMA-1/PS-1	285
PMMA-2/PS-2	11.3
PMMA-2/PS-3	0.3

remove the residual solvent. All blend samples were then stored in the freezer.

2.4. Isothermal annealing of rapidly precipitated specimens

Isothermal annealing experiment of rapidly precipitated blends was performed, due to its precise and accurate temperature control, using the Rheometrics mechanical spectrometer described above for rheological measurements. The as-precipitates were annealed at 170°C for various periods. Upon removal from the RMS fixture, all annealed precipitates were quenched in liquid nitrogen in order to freeze phase morphology stored in the freezer.

2.5. Transmission electron microscopy (TEM)

As-precipitates, after being annealed, were first embedded in an epoxy (EPON 828) and cured at room temperature using 10 wt% triethylenetetramine. Complete curing took about 24 h. The embedded samples were then ultramicrotomed at room temperature using a Reichert Ultracut S (Leica) microtome equipped with glass knives. Carbon black coating was applied to a PMMA/PS blend sample after ultramicrotoming. A transmission electron microscope (JEM 1200EX II, JEOL) operated at 100 kV was used to take micrographs of the PMMA/PS blend specimens.

3. Results

3.1. Morphology of PMMA/PS blends upon rapid precipitation from homogeneous solution

Fig. 1 gives TEM images of rapidly precipitated PMMA-1/PS-1 blends, Fig. 2 gives TEM images of rapidly precipitated PMMA-2/PS-2 blends, and Fig. 3 gives TEM images of rapidly precipitated PMMA-2/PS-3 blends, in which the white areas represent the PMMA phase and the dark areas represent the PS phase. In Figs 1–3 we observe a modulated co-continuous morphology in all three blend systems investigated. This can easily be understood when we recognize the fact that thermodynamically speaking, the phase separation mechanism involved with rapid precipitation (via composition quenching) is very similar to that involved with spinodal decomposition (via temperature quenching) [20–22].

In 1985 Inoue et al. [23] reported that they could not obtain a periodically-modulated morphology when PMMA and PS were cast from toluene, whereas they succeeded in obtaining a modulated co-continuous morphology for several other immiscible polymer pairs. They noted that a very fast evaporation of solvent was necessary to observe a modulated co-continuous morphology in an immiscible polymer blend from solvent casting. Such an observation seems to suggest that the type of solvent used for casting a pair of immiscible polymers plays an important role in obtaining a modulated co-continuous morphology. On the other hand, rapid precipitation does not require a removal of solvent. To the best of our knowledge, the present study is the first successful attempt made to obtain a modulated co-continuous morphology of PMMA/PS blend.

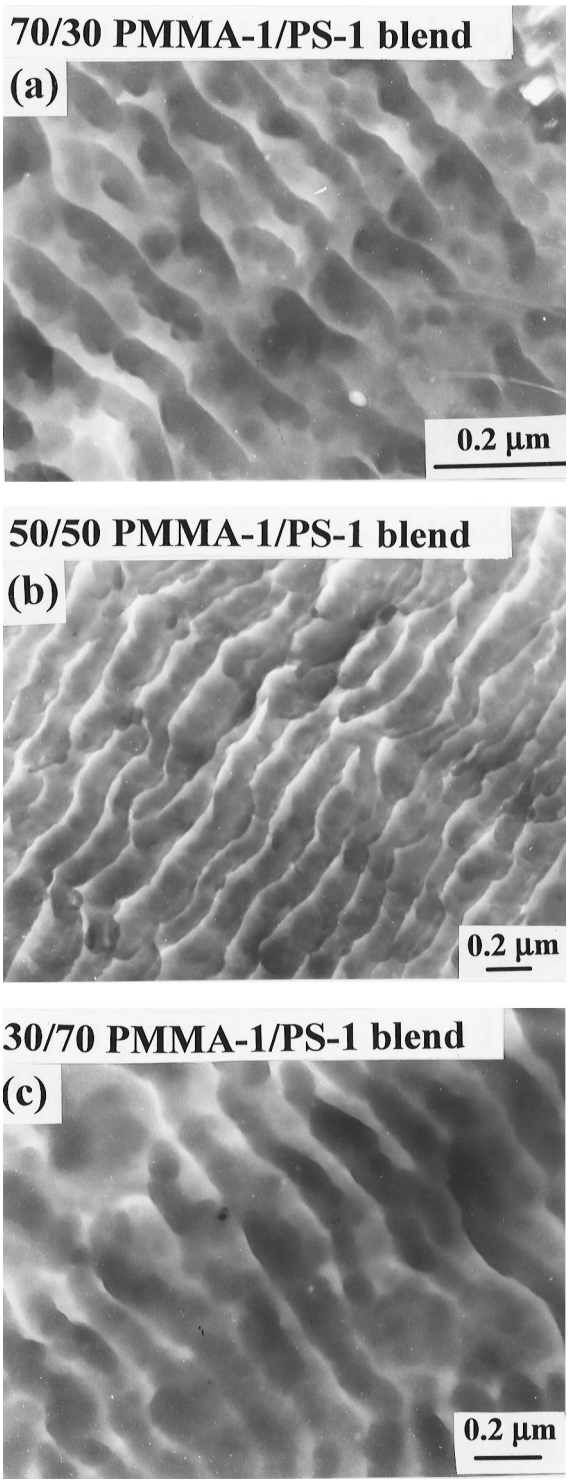

Fig. 1. TEM images of as-precipitated 70/30 PMMA-1/PS-1, 50/50 PMMA-1/PS-1, and 30/70 PMMA-1/PS-1 blends, showing a co-continuous morphology irrespective of blend composition.

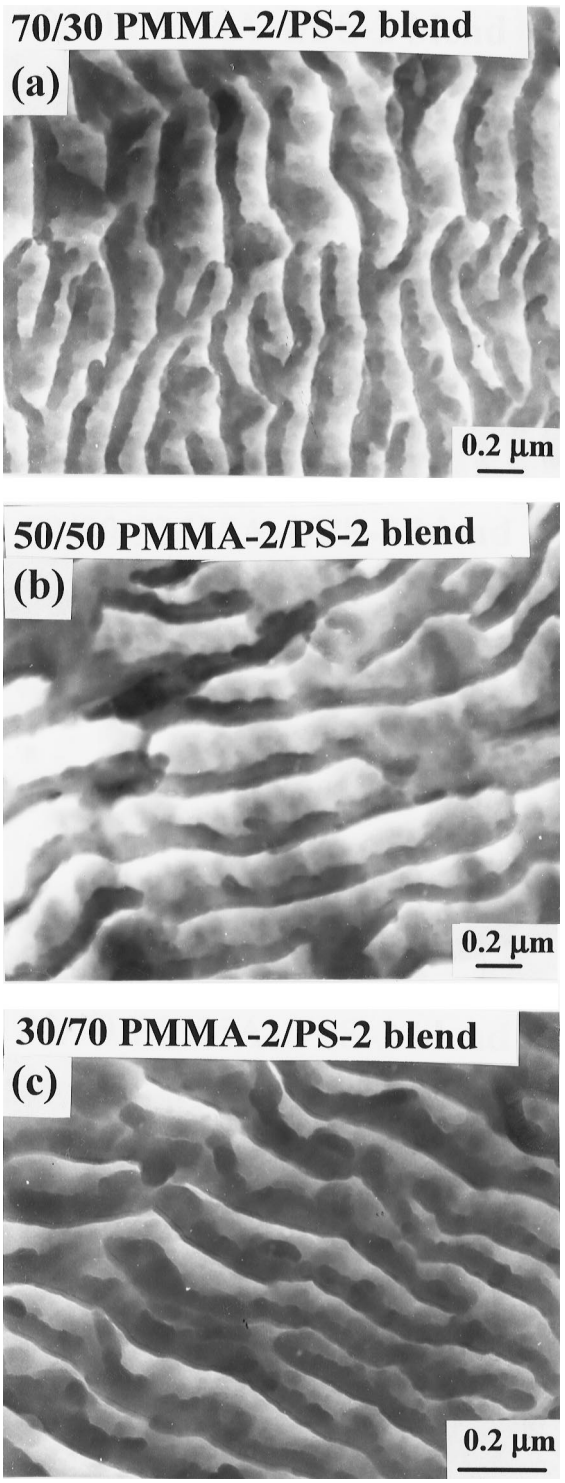

Fig. 2. TEM images of as-precipitated 70/30 PMMA-2/PS-2, 50/50 PMMA-2/PS-2, and 30/70 PMMA-2/PS-2 blends, showing a co-continuous morphology irrespective of blend composition.

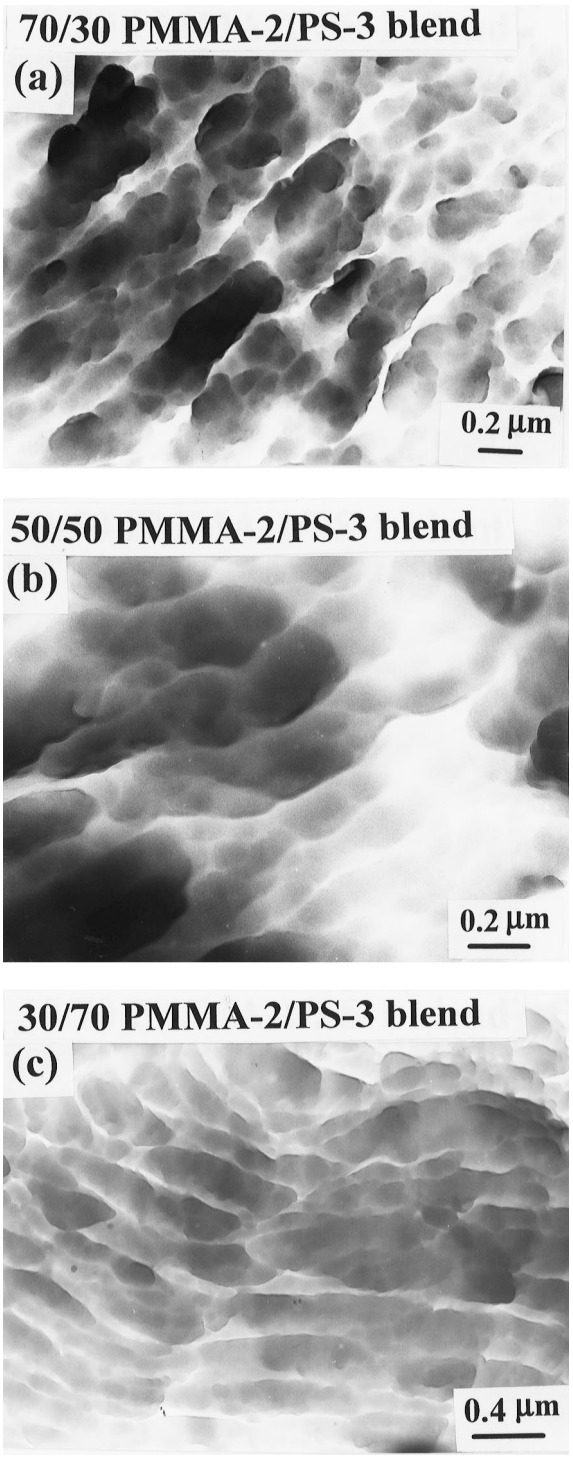

Fig. 3. TEM images of as-precipitated 70/30 PMMA-2/PS-3, 50/50 PMMA-2/PS-3, and 30/70 PMMA-2/PS-3 blends, showing a co-continuous morphology irrespective of blend composition.

In accordance with Cahn's theory of spinodal decomposition [20,21], the modulated co-continuous morphology observed in this study for PMMA/PS blends (see Figs 1–3) may be regarded as being formed by the superposition of the sine waves of thermal composition fluctuations. Fig. 4 gives a schematic representation, illustrating a three-dimensional, periodically modulated co-continuous structure, having the domain spacing Λ, for PMMA/PS blends obtained in this study by rapid precipitation. From the measurements of the distance between the centers of two adjacent modulated structures, we calculated Λ for

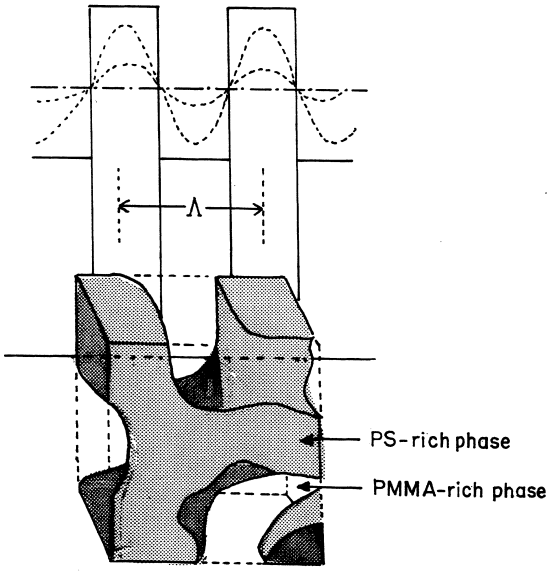

Fig. 4. A three-dimensional schematic representation of the periodically modulated co-continuous structure, formed via spinodal decomposition, and wavelength Λ of PMMA/PS blends.

PMMA-1/PS-1 blends using the TEM images given in Fig. 1 and for PMMA-2/PS-2 blends using the TEM images given in Fig. 2, and the results are summarized in Fig. 5. Owing to the unclear phase boundaries in Fig. 3, the values of Λ for the PMMA-2/PS-3 blends were not determined. The following observations are worth noting in Fig. 5. The value of Λ for an equal blend composition (50/50 PMMA/PA blend) is larger than that for the unequal blend compositions (30/70 and 70/30 PMMA/PS blends), and the PMMA-1/PS-1 blends (the symbol ○) have larger values of Λ than the PMMA-2/PS-2 blends (the symbol △). Below we will interpret the results using the Cahn's linearized theory [20,21].

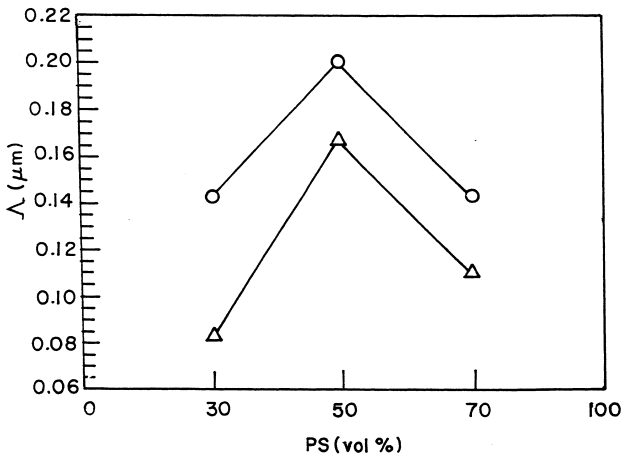

Fig. 5. Plots of Λ versus blend composition for PMMA/PS blends formed via spinodal decomposition: (○) PMMA-1/PS-1 blends: (△) PMMA-2/PS-2 blends.

3.2. Time evolution of the rapidly precipitated PMMA/PS blend morphology during isothermal annealing

Fig. 6 gives TEM images describing how, during isothermal annealing at 170°C, the morphology of a rapidly precipitated 70/30 PMMA-1/PS-1 blend specimen evolved with time from 5 min to 2 h. Fig. 7 gives TEM images describing the time evolution of a rapidly precipitated 70/30 PMMA-2/PS-2 blend, and Fig. 8 gives TEM images describing the time evolution of a rapidly precipitated 70/30 PMMA-2/PS-3 blend, when each blend was subjected to an isothermal annealing at 170°C for a period ranging from 5 min to 2 h. From Figs 6–8 we observe that (i) annealing at 170°C for 15 min was not long enough for us to observe a discernible change in blend morphology, (ii) prolonging the annealing time from 15 to 30 min enabled us to observe clearly that a modulated co-continuous morphology (see Figs 1a, 2a and 3a) evolved into a dispersed morphology, and (iii) prolonging the annealing time further to 2 h helped achieve a well-developed dispersed morphology in all three 70/30 PMMA-1/PS-1, 70/30 PMMA-2/PS-2, and 70/30 PMMA-2/PS-3 blends. Notice in Figs 6–8 that the minor component PS (the dark areas) formed the discrete phase and the major component PMMA (the white areas) formed the continuous phase.

Fig. 9 gives TEM images describing how, during isothermal annealing at 170°C, the morphology of a rapidly precipitated 30/70 PMMA-1/PS-1 blend specimen evolved with time from 30 min to 6 h. Fig. 10 gives TEM images describing the time evolution of a rapidly precipitated 30/70 PMMA-2/PS-2 blend, and Fig. 11 gives TEM images describing the time evolution of a rapidly precipitated 30/70 PMMA-2/PS-3 blend, when each blend was subjected to an isothermal annealing at 170°C for a period ranging from 30 min to 6 h. In Figs 9a, 10a and 11a we observe clearly that the modulated co-continuous morphology of 30/70 PMMA-1/PS-1 blend (Fig. 1c), 30/70 PMMA-2/PS-2 blend (Fig. 2c), and 30/70 PMMA-2/PS-3 blend (Fig. 3c), which was formed upon rapid precipitation of a homogeneous solution, did not evolve into a well-developed dispersed morphology after annealing for 30 min at 170°C, in contrast to the situations with 70/30 PMMA-1/PS-1 blend (Fig. 6c), 70/30 PMMA-2/PS-2 blend (Fig. 7c), and 70/30 PMMA-2/PS-3 blend (Fig. 8c). This observation indicates that the rate of morphology development is much slower in 30/70 PMMA/PS blends than in 70/30 PMMA/PS blends. Later in this paper we will offer an explanation on this experimental observation. As annealing continued to 6 h, in Figs 9c, 10c and 11c we observe that the minor component PMMA (the white areas) formed the discrete phase and the major component PS (the dark areas) formed the continuous phase.

Fig. 12 gives TEM images describing how, during isothermal annealing at 170°C, the morphology of a rapidly precipitated 50/50 PMMA-1/PS-1 blend specimen evolved with time from 30 min to 12 h. Fig. 13 gives TEM images

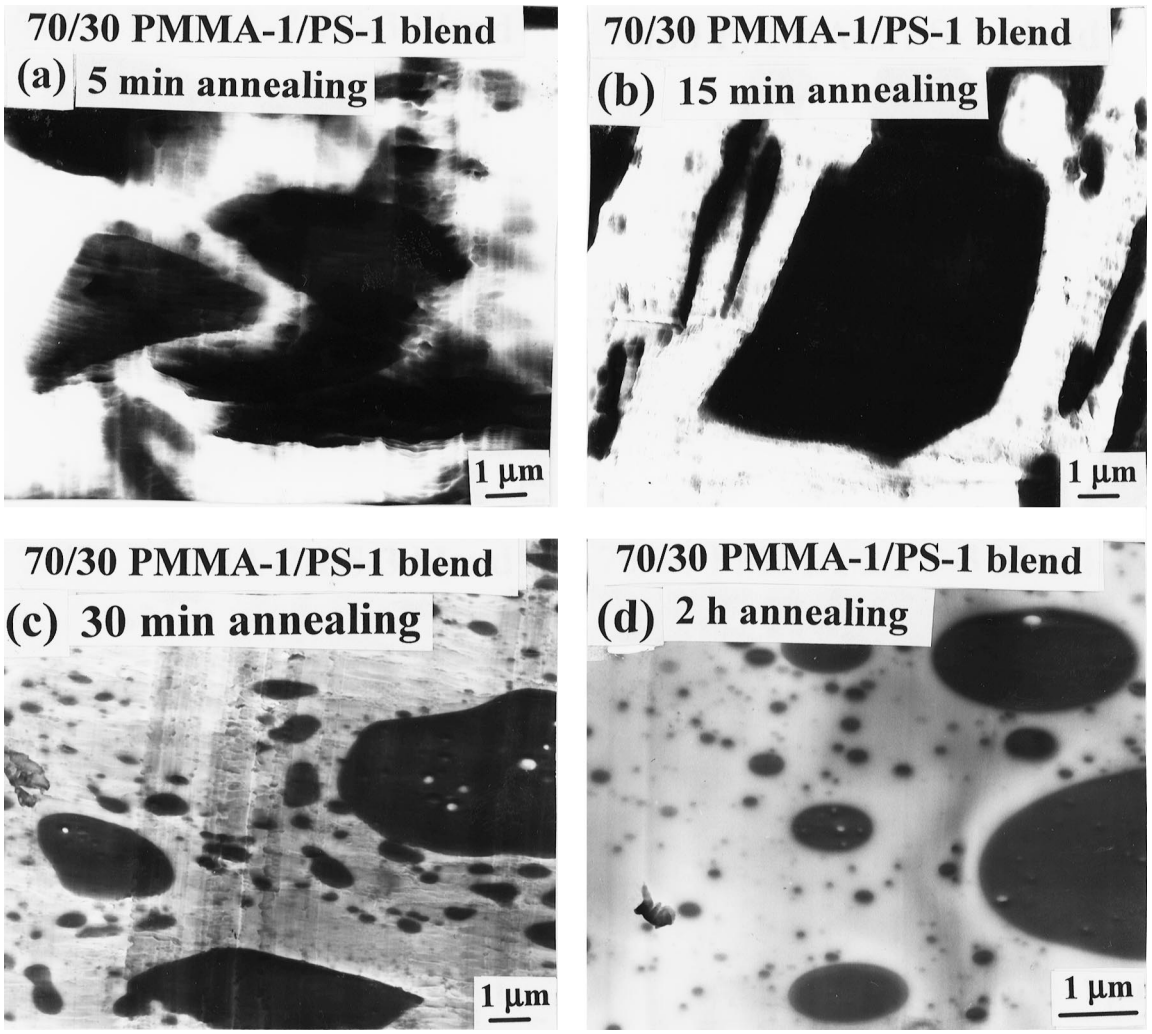

Fig. 6. TEM images of a rapidly precipitated 70/30 PMMA-1/PS-1 blend after being annealed at 170°C for: (a) 5 min; (b) 15 min; (c) 30 min; (d) 2 h.

describing the time evolution of a rapidly precipitated 50/50 PMMA-2/PS-2 blend, and Fig. 14 gives TEM images describing the time evolution of a rapidly precipitated 50/50 PMMA-2/PS-3 blend, when each blend was subjected to an isothermal annealing at 170°C for a period ranging from 30 min to 12 h. It is not clear in Figs 12–14 how the morphology evolved during the annealing period of 30 min. As annealing continued to 2 h, as shown in Figs 12b, 13b and 14b, the morphology of 50/50 PMMA/PS blends developed, showing more or less a 'dual mode' of dispersed morphology, namely, a region exists where PS formed the discrete phase dispersed in the PMMA matrix and another region also exists where PMMA formed the discrete phase dispersed in the PS matrix. When annealing continued to 12 h at 170°C, in Figs 12d, 13d and 14d we observe a well-developed 'dual mode' of dispersed morphology which started from a modulated co-continuous morphology (see Figs 1b, 2b and 3b). Such a seemingly complicated blend morphology apparently is unique to equal blend composition.

3.3. Effect of shear flow on the morphology of rapidly precipitated PMMA/PS blend

Fig. 15 gives TEM images of the morphology (the upper panel) of 50/50 PMMA-1/PS-1 blend and, also, the morphology (the lower panel) of 50/50 PMMA-2/PS-3 blend, each of which was obtained by extruding a rapidly precipitated specimen in a capillary die at 220°C at a shear rate of 260 s^{-1}. In Fig. 15 we observe that the extrudate of 50/50 PMMA-1/PS-1 blend has PMMA droplets (the white areas) dispersed in the PS matrix (the dark areas) and the extrudate of 50/50 PMMA-2/PS-3 blend has PS droplets (the dark areas) dispersed in the PMMA matrix (the white areas). Fig. 16 describes the shear dependence of viscosity at 220°C for PMMA-1, PS-1, PMMA-2, and PS-3, showing that over the entire range of shear rates investigated, PMMA-1 (the symbol △) has viscosities higher than PS-1 (the symbol ○), and PS-3 (the symbol ●) has viscosities higher than PMMA-2 (the symbol ▲). We can then conclude from Figs 15 and 16 that for an equal volume fraction of the constituent components, the more viscous component

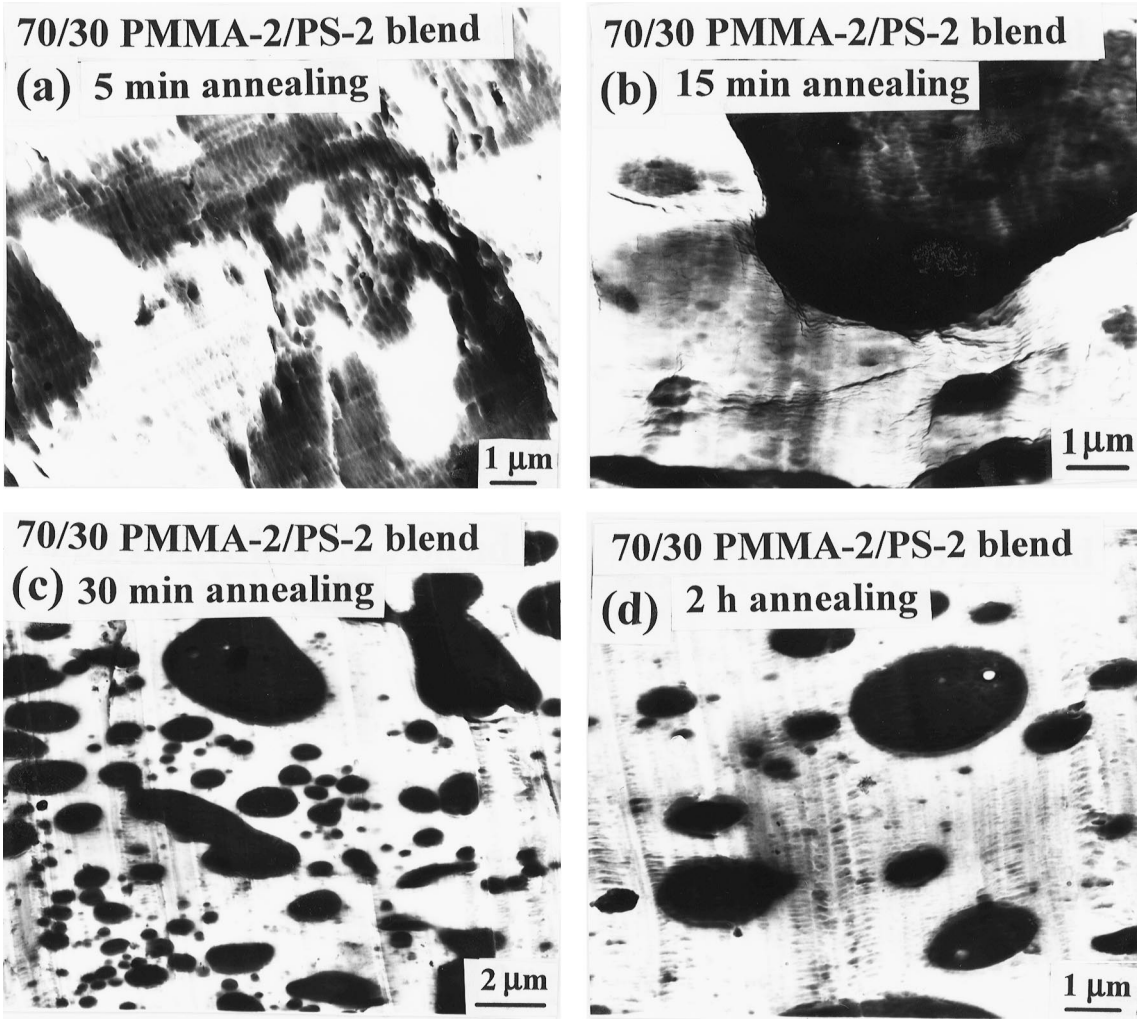

Fig. 7. TEM images of a rapidly precipitated 70/30 PMMA-2/PS-2 blend after being annealed at 170°C for: (a) 5 min; (b) 15 min; (c) 30 min; (d) 2 h.

forms the discrete phase dispersed in the less viscous component, i.e. the viscosity ratio determines the state of dispersion (which of the two components, PS or PMMA, forms the discrete phase dispersed in the other component).

4. Discussion

Let us interpret the experimental results presented above using currently held theories. The time evolution of the phase-separated structures of polymer mixtures obtained by spinodal decomposition may be divided into three stages: (i) the early stage, (ii) the late stage, and (iii) the final stage. In the past, the early stage of spinodal decomposition was interpreted using the theory of Cahn [20,21], who first derived the following expression for the composition ϕ_A in an inhomogeneous mixture consisting of components A and B,

$$\frac{\partial \phi_A}{\partial t} = M\left(\frac{\partial^2 f(\phi_A)}{\partial \phi_A^2}\nabla^2\phi_A - 2\kappa\nabla^4\phi_A\right) \tag{1}$$

where $f(\phi_A)$ is the free energy density of homogeneous material of composition ϕ_A, κ is the gradient energy coefficient arising from the effects of localized composition gradient, and M is the mobility defined by the ratio of diffusion flux ($\mathbf{J}_B$ or $\mathbf{J}_A$) to the gradient of chemical potential, $\mu_A - \mu_B$,

$$\mathbf{J}_B = -\mathbf{J}_A = M\nabla(\mu_A - \mu_B) \tag{2}$$

Note that Eq. (1) is very similar to the conventional diffusion equation with diffusion coefficient D if we define $D_c = M|\partial^2 f/\partial\phi_A^2|$ in Eq. (1). Note that $D_c \neq D$ and D_c is called the cooperative (or apparent) diffusion coefficient. The solution of Eq. (1) may be written as [20,21]

$$\phi_A \propto e^{R(\beta)t} \tag{3}$$

where

$$R(\beta) = -D_c\beta^2 - 2M\kappa\beta^4 \tag{4}$$

in which β is the wavenumber defined by $\beta = 2\pi/\Lambda$ with Λ being the wavelength or domain spacing.

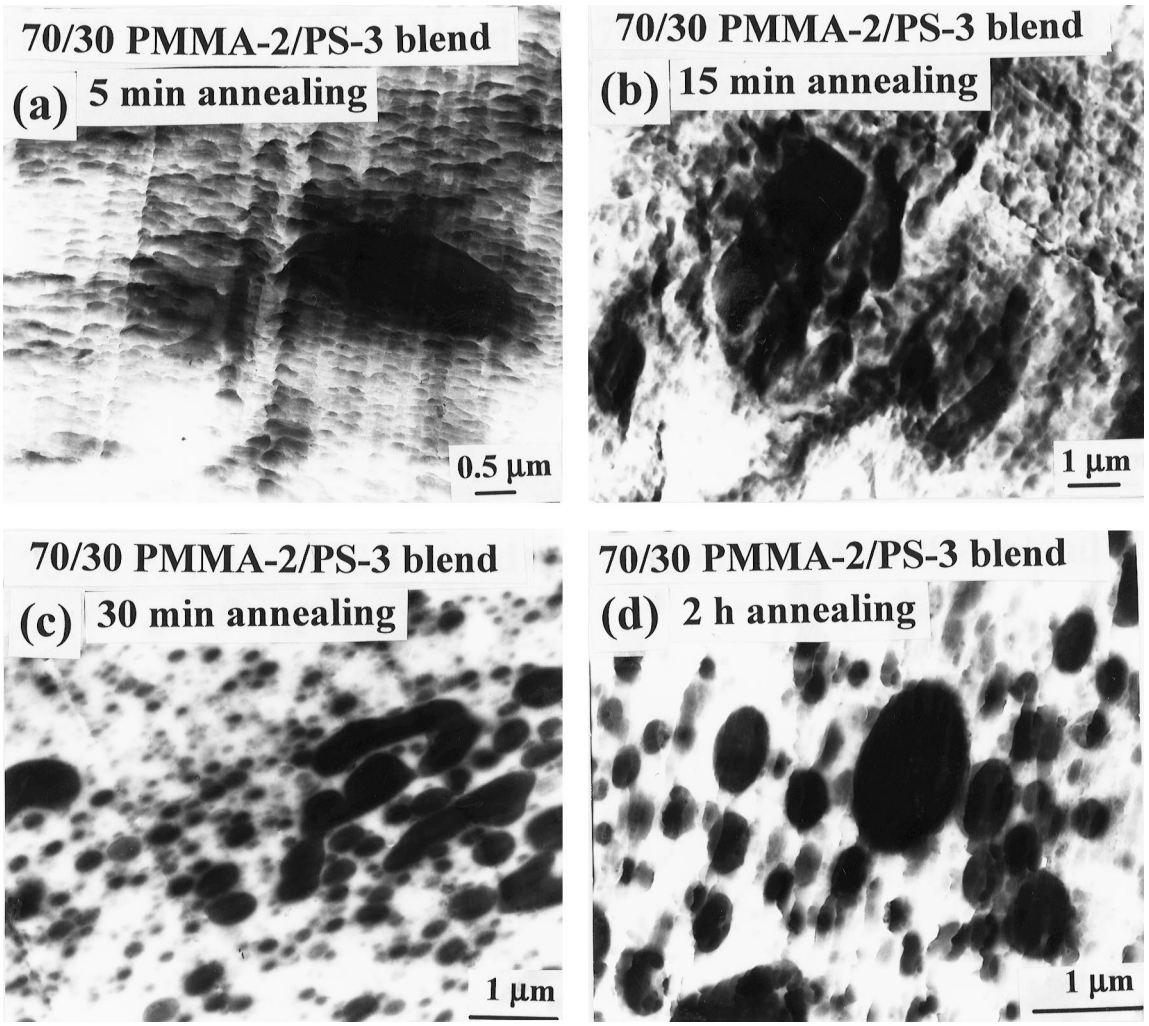

Fig. 8. TEM images of a rapidly precipitated 70/30 PMMA-2/PS-3 blend after being annealed at 170°C for: (a) 5 min; (b) 15 min; (c) 30 min; (d) 2 h.

According to the Cahn's linearized theory [20,21], the growth rate of concentration fluctuations in terms of the volume fraction of the total polymer, $\phi_p(t)$, in a ternary system consisting of a pair of immiscible polymers and a solvent is given by [23]

$$|\phi_p(t) - \phi_p(0)| \propto e^{R_m t} \tag{5}$$

where $\phi_p(0)$ is the volume fraction of the total polymer in the initially homogeneous solution and R_m is the maximum rate constant of concentration fluctuation growth at β_m, which is the value of β at $\{\partial R(\beta)/\partial\beta\}|_{\beta=\beta_m} = 0$, with $\beta_m = 2\pi/\Lambda_m$ where Λ_m is the maximum wavelength. $R_m(t)$ and $\Lambda_m(t)$, respectively, are related to the polymer concentrations ϕ_p by [23]

$$\Lambda_m(t) \propto (\phi_p - \phi_p^s)^{-1/2} \tag{6}$$

$$R_m(t) \propto M\frac{\chi_{AB}}{N_A}\phi_p(\phi_p - \phi_p^s)^2 \tag{7}$$

where ϕ_p^s is the polymer concentration at the point of spinodal decomposition and it is given by

$$\phi_p^s = \frac{N_A}{2\chi_{AB}}\left(\frac{1}{N_A\theta_A} + \frac{1}{N_B\theta_B}\right) \tag{8}$$

in which χ_{AB} is the Flory–Huggins interaction parameter, N_A and N_B are degrees of polymerization for polymers A and B, respectively, $\theta_A = \phi_A/(\phi_A + \phi_B)$ is the volume fraction of polymer A, $\theta_B = \phi_B/(\phi_A + \phi_B)$ is the volume fraction of polymer B, and $\phi_p = \phi_A + \phi_B = 1 - \phi_S$ with ϕ_S being the volume fraction of solvent in the ternary mixture.

The following observation can be made from Eqs. (6) and (8). For given molecular weights of the component polymers (i.e. for fixed values of N_A and N_B), from Eq. (8) we have a minimum value of ϕ_p^s at $\theta_A = \theta_B = 0.5$, thus from Eq. (6) we have the longest periodic distance of modulated structure. This observation now explains the experimental results given in Fig. 5, the largest value of Λ for the 50/50 PMMA-1/PS-1 and 50/50 PMMA-2/PS-2 blends. For a given blend composition (i.e. for given values of θ_A and θ_B), it follows from Eq. (8) that ϕ_p^s will decrease with

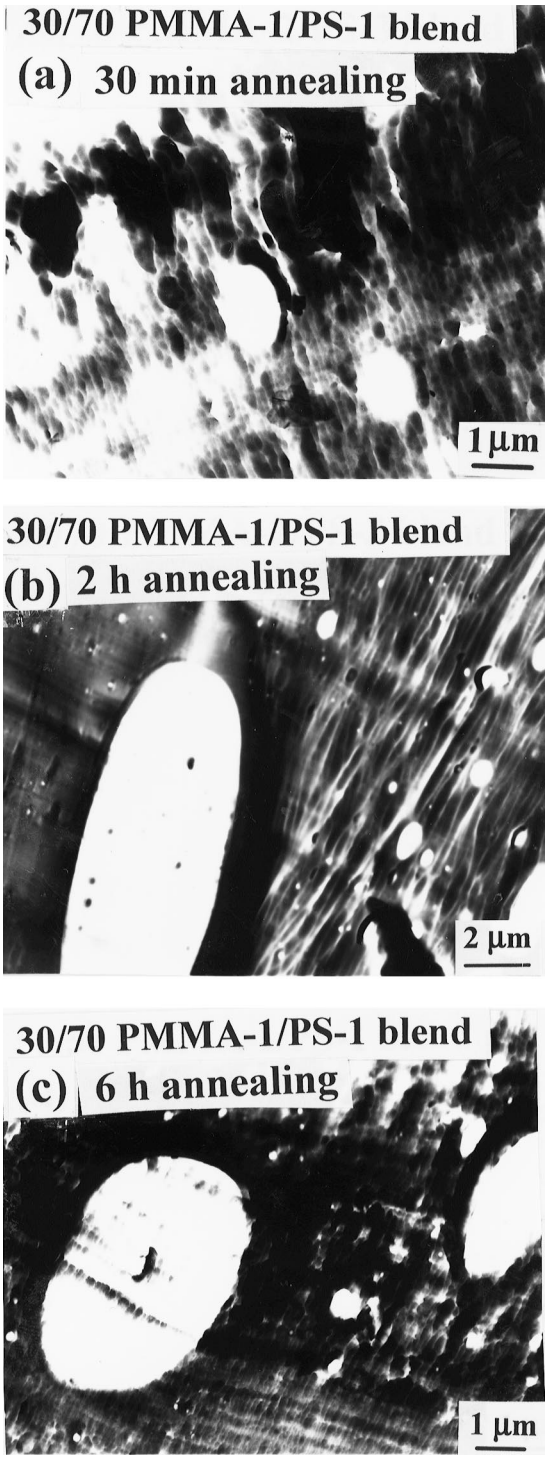

Fig. 9. TEM images of a rapidly precipitated 30/70 PMMA-1/PS-1 blend after being annealed at 170°C for: (a) 30 min; (b) 2 h; (c) 6 h.

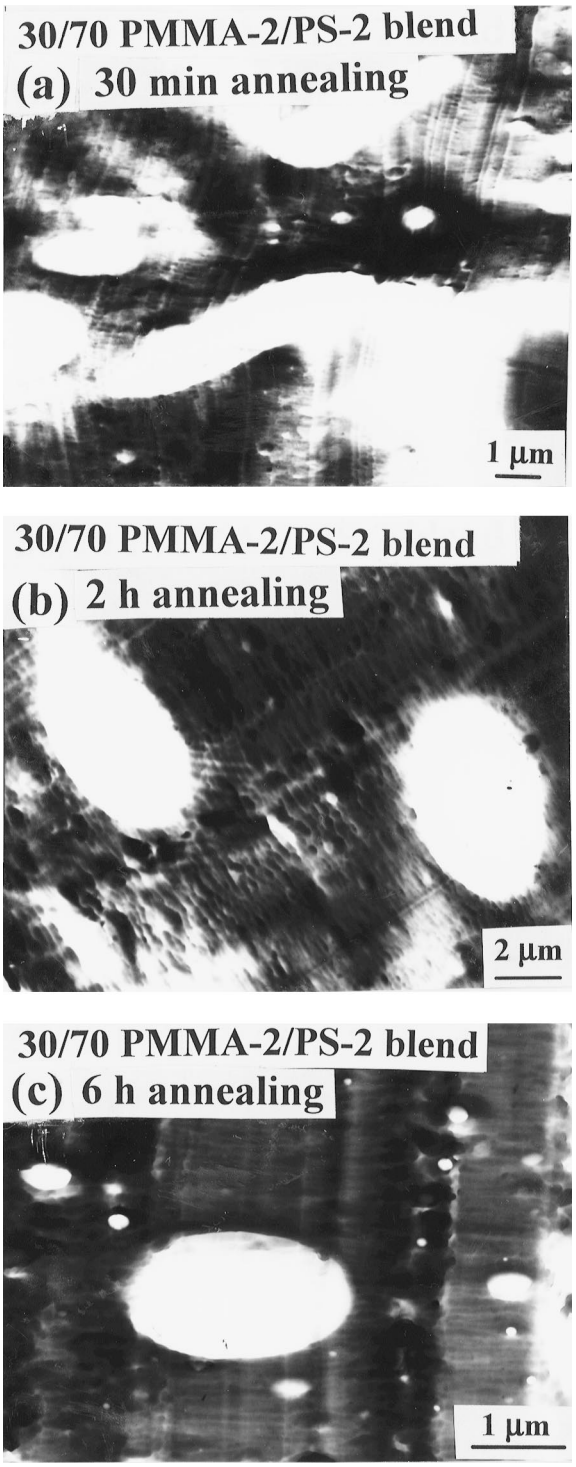

Fig. 10. TEM images of a rapidly precipitated 30/70 PMMA-2/PS-2 blend after being annealed at 170°C for: (a) 30 min; (b) 2 h; (c) 6 h.

increasing molecular weight (N_A or N_B) of polymers *A* and *B*, indicating that, in accordance with Eq. (6), the higher the molecular weights of the component polymers, the larger the value of Λ_m will be. This observation now explains the experimental results in Fig. 5: the PMMA-1/PS-1 blends with higher molecular weights (the symbol ○) have larger values of Λ than the PMMA-2/PS-2 blends (the symbol △) (see Table 1 for the molecular weights of the components).

In the past, a number of research groups [22–25] investigated, via light scattering, the kinetics of phase separation of binary polymer blends and reported that the Cahn's linearized theory describes well the initial stage of spinodal decomposition. Hashimoto and coworkers [26–32]

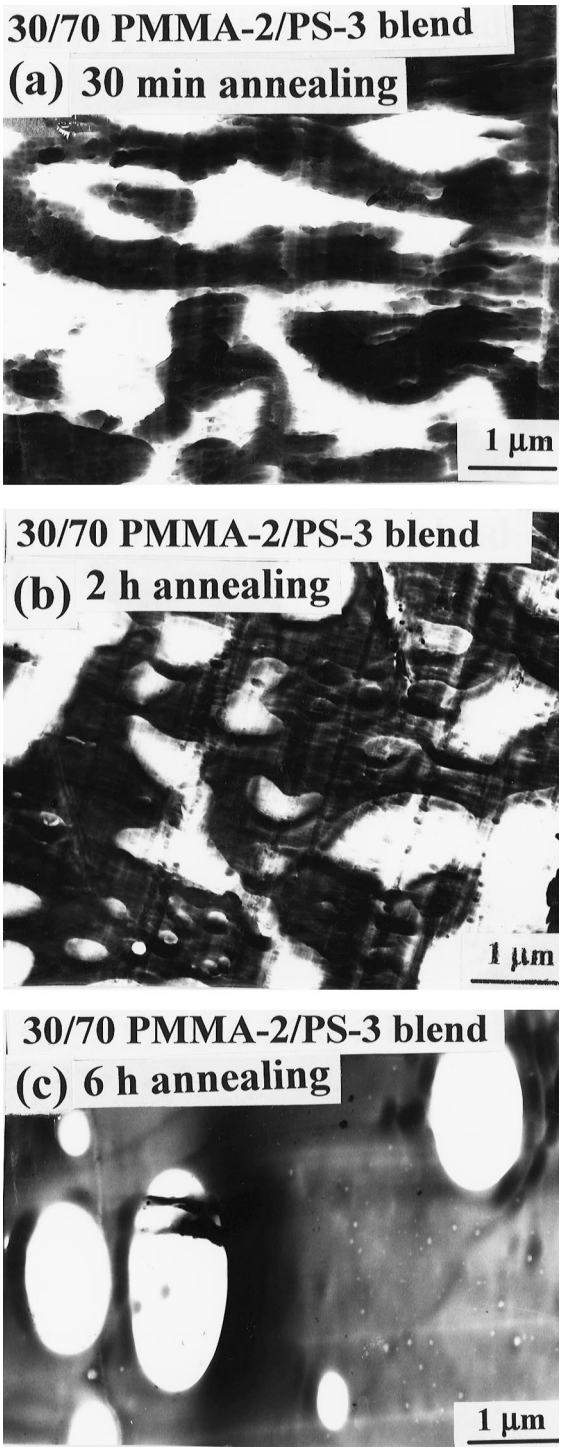

Fig. 11. TEM images of a rapidly precipitated 30/70 PMMA-2/PS-3 blend after being annealed at 170°C for: (a) 30 min; (b) 2 h; (c) 6 h.

conducted, via time-resolved light scattering, an extensive investigation of late stages of spinodal decomposition of polymer blends, which were obtained by either rapid quenching or solvent casting. Hashimoto and coworkers [27,31] proposed the percolation-to-cluster transition (PCT) mechanism to interpret their experimental results. According to the PCT mechanism, the modulated co-continuous morphology may be regarded as being in a state of 'percolation'. As phase separation progresses (e.g. by isothermal annealing in the present study) in an asymmetric blend composition, a phase rich in the minor component cannot maintain percolation and hence a continuity of the modulated co-continuous structure in three-dimensional space is broken, resulting in fragments (later becoming droplets) of the minor component, and they are dispersed in the matrix of the major component. Hence, the evolution from a modulated co-continuous morphology into a dispersed morphology in binary polymer blends, observed in the present study (see Figs 6–11), appears to fit in the PCT mechanism of Hashimoto et al. [27,31] However, during isothermal annealing of the symmetric blend composition, we observed a 'dual mode' of dispersed morphology as shown in Figs 12–14. Below we will offer an explanation on the formation of such blend morphology for the symmetric blend composition.

According to the PCT mechanism, the state of dispersion (which of the two components, PS or PMMA, forms the discrete or continuous phase in the present study) in the cluster regime depends on the volume fraction of the constituent components; namely, in a blend having off-critical blend composition the minor component will form the discrete phase and the major component will form the continuous phase. This observation now explains (i) why the modulated co-continuous morphology, initially formed via rapid precipitation from a 70/30 PMMA/PS mixture (see Figs 1a, 2a and 3a), evolved, under isothermal annealing at 170°C for a sufficiently long time (say 2 h), into a dispersed morphology in which the minor component PS formed droplets dispersed in the PMMA matrix (see Figs 6d, 7d and 8d), and (ii) why the modulated co-continuous morphology, initially formed via rapid precipitation from a 30/70 PMMA/PS mixture (see Figs 1c, 2c and 3c), evolved, under isothermal annealing at 170°C for a sufficiently long time (say 6 h), into a dispersed morphology in which the minor component PMMA formed droplets dispersed in the PS matrix (see Figs 9c, 10c and 11c).

It should be mentioned that the time evolution of the rapidly precipitated blend morphology during isothermal annealing, presented in Figs 6–14, can be regarded as being equivalent to late stages of spinodal decomposition. While periodic concentration fluctuations develop in the early stage of spinodal decomposition and are diffusion-controlled, breakdown of a periodically modulated co-continuous structure in later stages of spinodal decomposition is driven by the surface tension at rates controlled by the viscosity of the phases. The phase volumes in late stages of spinodal decomposition are determined by a co-existence curve of the mixture, phase separation temperature and composition. According to the PCT mechanism, there exist percolation limits beyond which a modulated co-continuous morphology starts to evolve into a dispersed morphology. Hence, percolation limits are equivalent to the existence of a critical domain size d_c, above which the

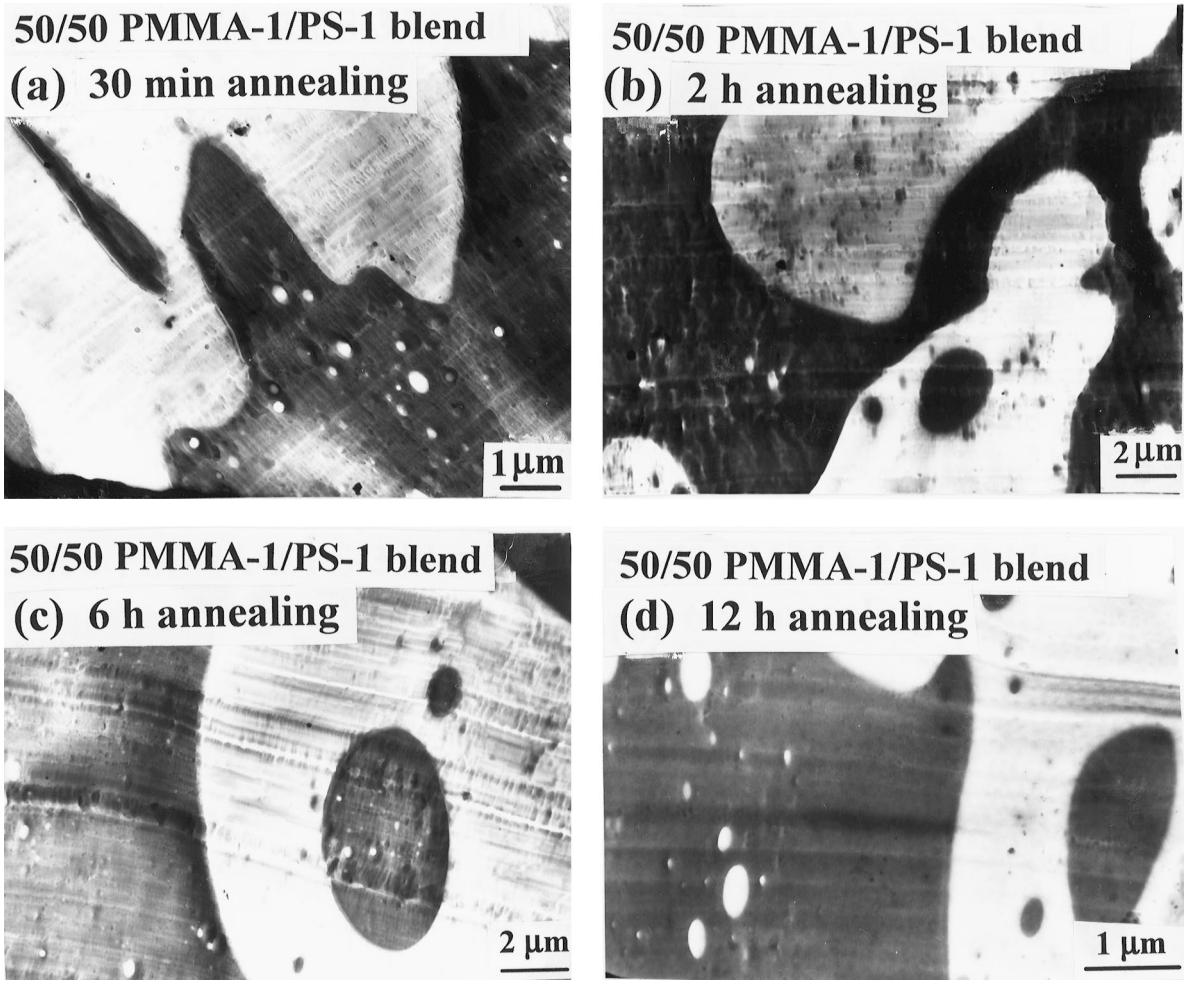

Fig. 12. TEM images of a rapidly precipitated 50/50 PMMA-1/PS-1 blend after being annealed at 170°C for: (a) 30 min; (b) 2 h; (c) 6 h; (d) 12 h.

mixture breaks up into irregularly shaped morphology, which then coarsens. According to Takeno and Hashimoto [32], breakup of a modulated co-continuous morphology may be driven by the capillary pressure involved in the structure: a thick part of the structure having a large cross section has a capillary pressure lower than a thin part having smaller cross section, generating a pressure gradient which then may cause flow from the thin part towards the thick part.

A theoretical investigation of late stages of spinodal decomposition was first carried out by Siggia [33], who showed that the hydrodynamic effects are very important and that the domain size (d) grows following two mechanisms: (i) $d \propto (k_B T/\eta_o)^{1/3} t^{1/3}$ in the early stage, which is governed by hydrodynamic effects and diffusion, where $k_B T$ represents thermal energy with k_B being the Boltzmann constant and η_o is the zero-shear viscosity, and (ii) $d \propto (\gamma/\eta_o)t$ in the long-term coarsening which is driven by the interfacial tension γ at a rate controlled by the viscosity η_o.

Using Siggia's analysis [33], we can now explain the experimental results presented in Figs 6–14, namely, the time evolution of a modulated co-continuous morphology into a dispersed morphology during isothermal annealing at 170°C. Although, during isothermal annealing, there was no bulk flow in the rapidly precipitated blend specimen, according to Siggia's analysis [33], the zero-shear viscosity must have played an important role in controlling the growth rate of domain $d(t)$. Note that the diffusion coefficient (D_c) (or mobility M) is related to the zero-shear viscosity (η_o), which in turn depends on the molecular weight (M_w) of the constituent components. Thus we have

$$d(t) \propto D_c \propto M \propto \frac{\gamma}{\eta_0} \propto \frac{\gamma}{M_w^{3.4}} \tag{9}$$

in which the polymers under consideration are assumed to be entangled. At 170°C we have the following relationships: $\eta_{o,PMMA\text{-}1} > \eta_{o,PS\text{-}1}$ and $\eta_{o,PMMA\text{-}2} > \eta_{o,PS\text{-}2}$ (see Tables 2 and 3). We can now explain why the rate of evolution of the dispersed morphology in 70/30 PMMA-1/PS-1 and 70/30 PMMA-2/PS-2 blends (see Figs 6c and 7c), in which the minor component PS forms the discrete phase dispersed in the major component PMMA, is faster than that in 30/70 PMMA-1/PS-1 and 30/70 PMMA-2/PS-2 blends (see Figs 9c and 10c), in which the minor component PMMA forms the discrete phase dispersed in the major component PS.

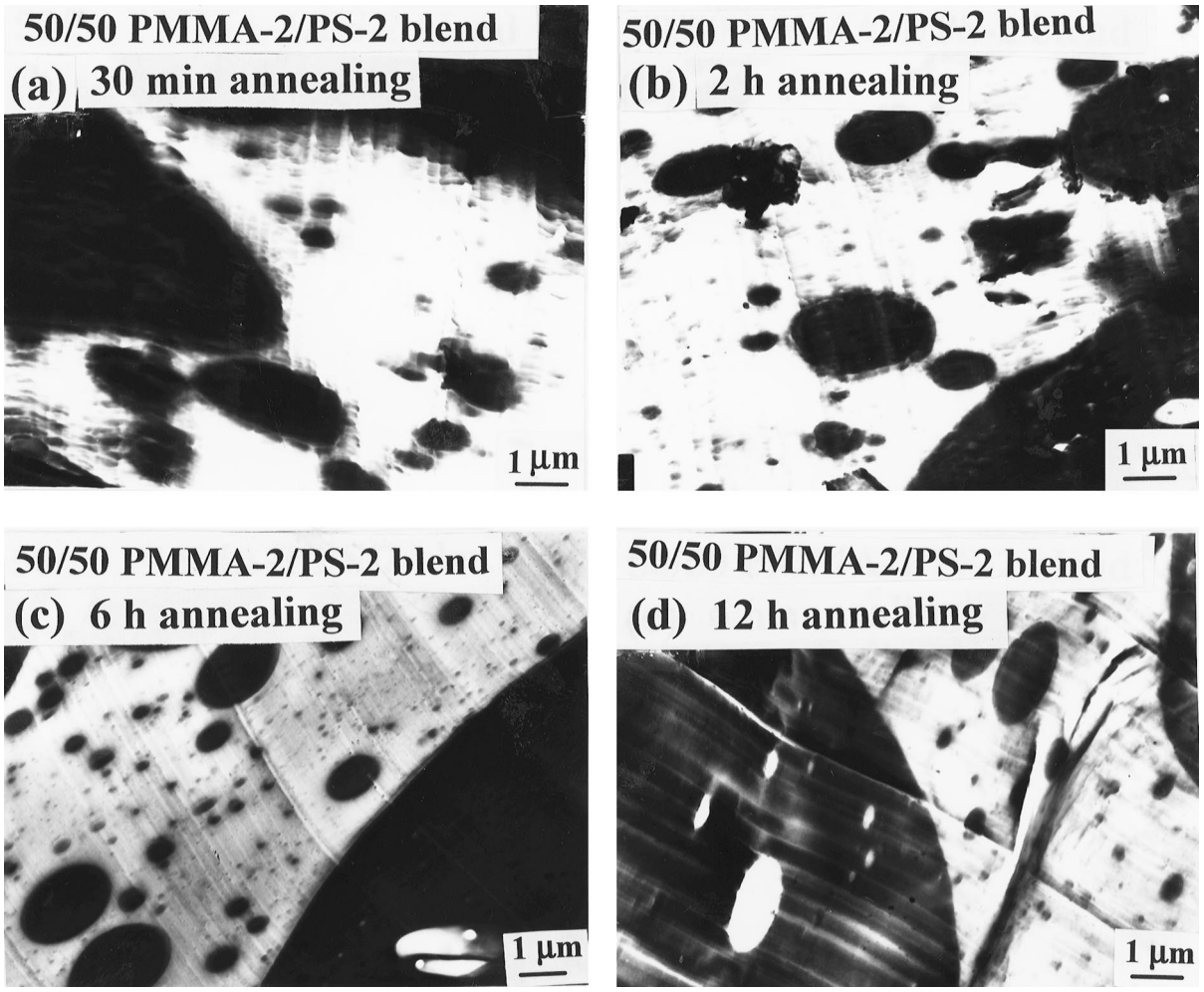

Fig. 13. TEM images of a rapidly precipitated 50/50 PMMA-2/PS-2 blend after being annealed at 170°C for: (a) 30 min; (b) 2 h; (c) 6 h; (d) 12 h.

Having explained above that the zero-shear viscosity played an important role in determining the state of dispersion during isothermal annealing of a rapidly precipitated PMMA/PS blend, we would like to revisit the state of dispersion in asymmetric PMMA/PS blend compositions. Specifically, in Figs 6–8 we observe that the major component PMMA forms the continuous phase and the minor component PS forms the discrete phase, and in Figs 9–11 we observe that the major component PS forms the continuous phase and the minor component PMMA forms the discrete phase, regardless of the viscosity ratio of the constituent components (see Tables 2 and 3). The above observation led us to conclude that the blend composition played a predominant role over the viscosity ratio in determining the state of dispersion during isothermal annealing of a rapidly precipitated PMMA/PS blend. From the point of view of the minimum energy dissipation principle, which is applicable to bulk flow of a two-phase liquid, we expect that the less viscous component will form the continuous phase and the more viscous component will form the discrete phase. Having realized the fact that isothermal annealing employed in the present study did not involve bulk flow, we can easily surmise that the minimum energy dissipation principle would not be applicable to the present study. Nevertheless, in order to ensure that the experimental observations made above are unambiguous, we prepared via rapid precipitation two additional blends, 60/40 and 55/45 PMMA-1/ PS-1 blends, lying between 70/30 and 50/50 PMMA-1/PS-1 blends, which were then annealed at 170°C for various periods.

In Fig. 17 the upper panel gives TEM images describing the morphology evolution of a rapidly precipitated 60/40 PMMA-1/PS-1 blend specimen, and the lower panel gives TEM images describing the morphology evolution of a rapidly precipitated 55/45 PMMA-1/PS-1 blend specimen, during isothermal annealing at 170°C for a period ranging from 30 min to 6 h. It is clear from Fig. 17 that the major component PMMA-1 forms the continuous phase and the minor component PS-1 forms the discrete phase although at 170°C PMMA-1 is much more viscous than PS-1 (see Tables 2 and 3). The above observation reassured us that when there is no bulk flow as in the present study, the blend composition plays a predominant role over the viscosity ratio of the constituent components in determining the

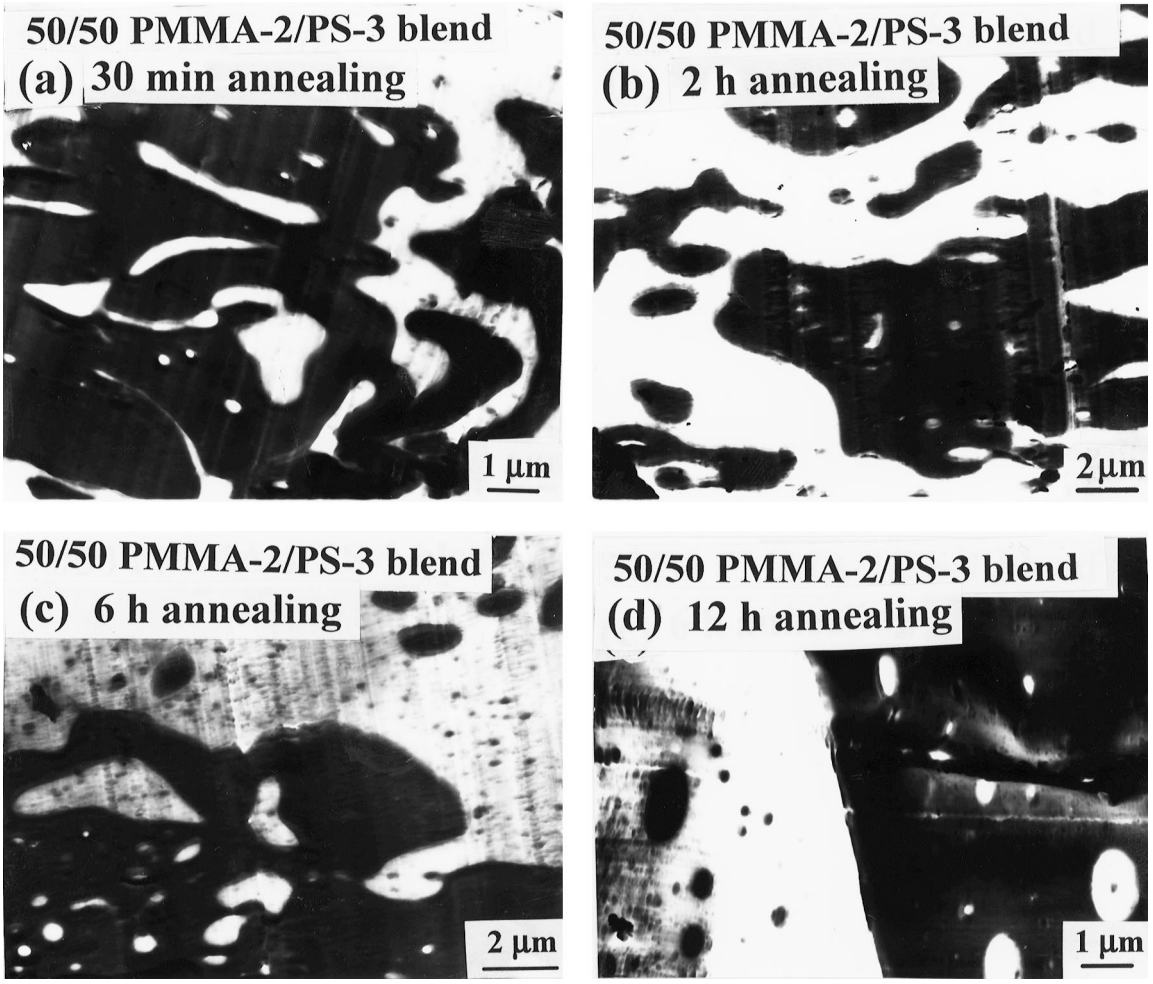

Fig. 14. TEM images of a rapidly precipitated 50/50 PMMA-2/PS-3 blend after being annealed at 170°C for: (a) 30 min; (b) 2 h; (c) 6 h; (d) 12 h.

state of dispersion, consistent with the PCT mechanism of Hashimoto et al. [27,31].

Now, we would like to offer an explanation on the differences observed in the morphology evolution of the symmetric PMMA/PS blend composition with bulk flow (see Fig. 15) and without bulk flow (see Figs 12–14). Specifically, the readers are reminded that in Fig. 15 we have shown a well-developed dispersed morphology when a rapidly precipitated 50/50 PMMA-1/PS-1 blend, which initially formed a co-continuous morphology, was extruded in a capillary die at 220°C. In Figs 12–14 we have shown a 'dual mode' of dispersed morphology when the blend was annealed under isothermal conditions at 170°C for 12 h. The difference between the two situations lies in that in the former, morphology evolution took place during bulk flow, whereas in the latter, morphology evolution took place under quiescent conditions. In the presence of bulk flow, the minimum energy dissipation principle plays the role in determining the state of dispersion, thus giving rise to a well-dispersed morphology in which the less viscous component forms the continuous phase and the more viscous component forms the discrete phase. As pointed out above, in the absence of bulk flow, the minimum energy dissipation principle is not applicable and thus the blend composition is expected to determine the state of dispersion. However, when a symmetric blend (i.e. 50/50 PMMA/PS blend) is subjected to isothermal annealing under quiescent conditions, the blend composition is not expected to determine the state of dispersion. Under such a situation, the PCT mechanism prevails. Since the co-continuous morphology formed initially upon rapid precipitation of a homogeneous solution does not have perfectly aligned lamellae (see Figs 1–3), local movement of each phase during isothermal annealing under quiescent conditions, in accordance with the PCT mechanism, appears to have determined the state of dispersion, giving rise to a 'dual mode' of dispersion.

5. Concluding remarks

In this study we were successful in observing a periodically modulated co-continuous morphology, irrespective of blend ratio, when a homogeneous solution of PMMA and PS was rapidly precipitated in a non-solvent. We have demonstrated that phase separation by rapid precipitation via composition quenching is equivalent to that by spinodal

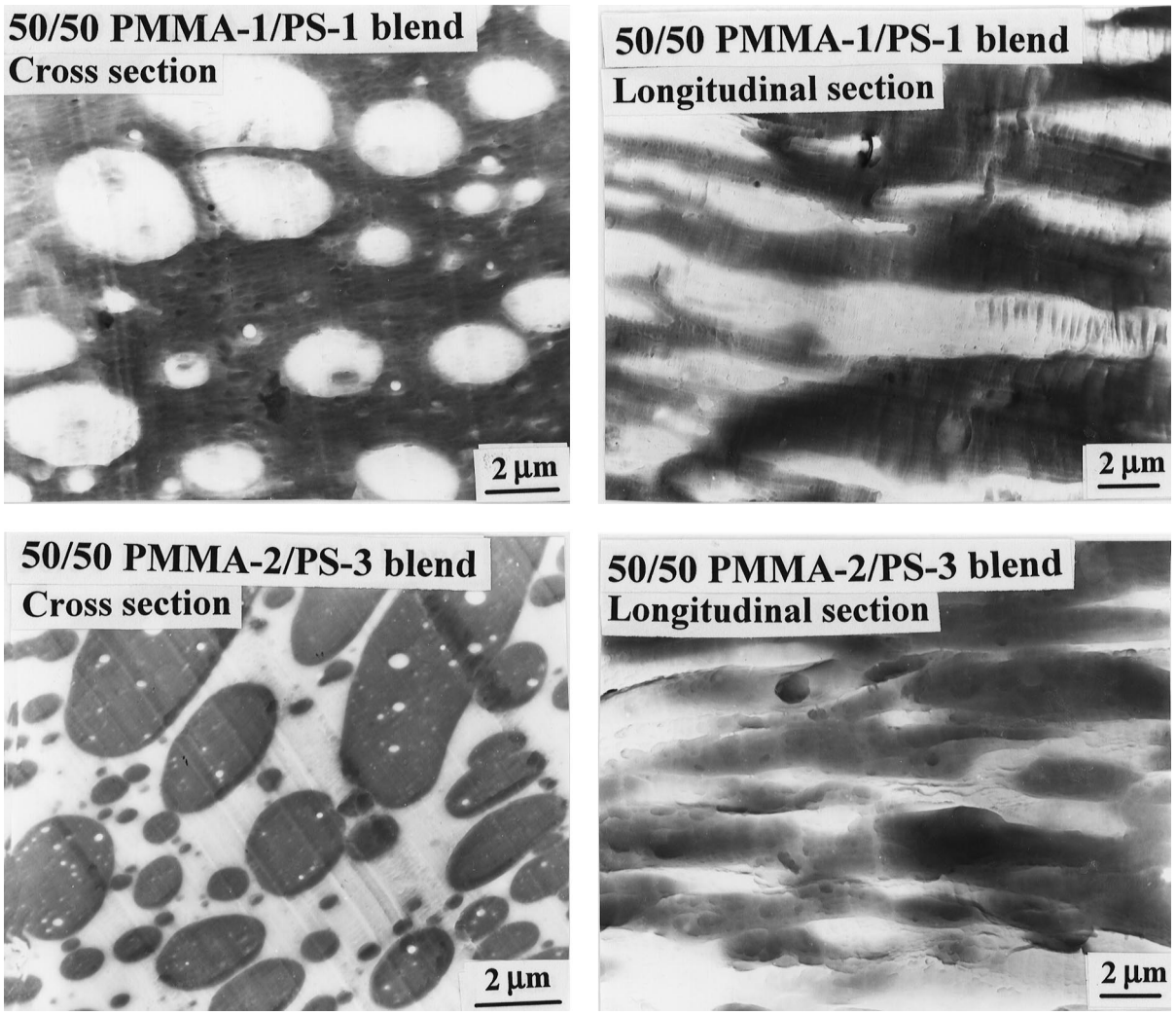

Fig. 15. The upper panel shows TEM images of a rapidly precipitated 50/50 PMMA-1/PS-1 blend after being extruded in a capillary at 220°C at a shear rate of 260 s^{-1}. The lower panel shows TEM images of a rapidly precipitated 50/50 PMMA-2/PS-3 blend after being extruded in a capillary at 220°C at a shear rate of 260 s^{-1}.

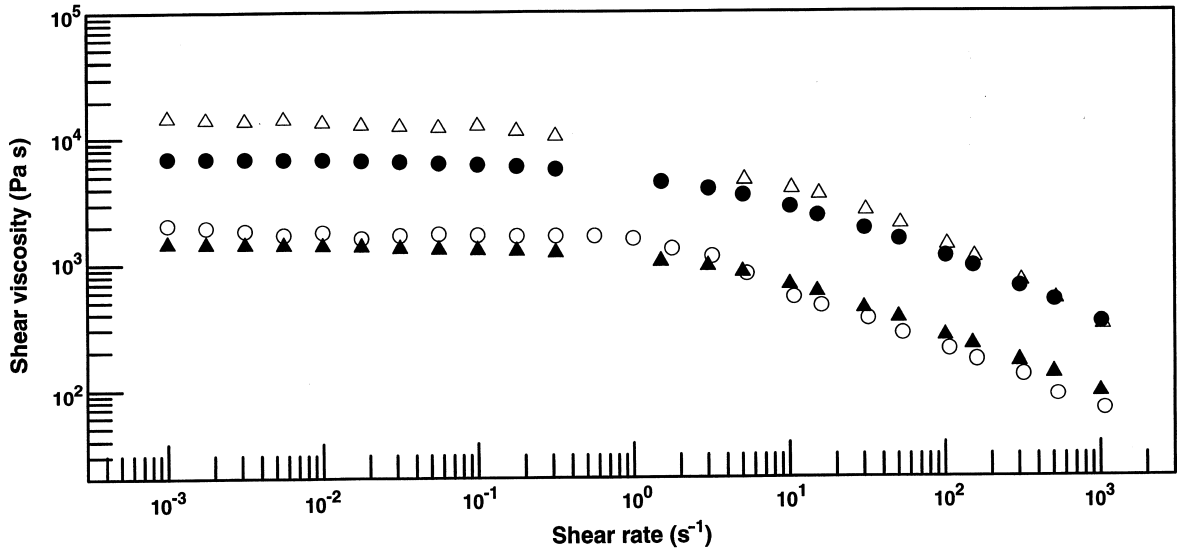

Fig. 16. Logarithmic plots of shear viscosity versus shear rate at 220°C for: (△) PMMA-1, (○) PS-1, (▲) PMMA-2, and PS-3 (●).

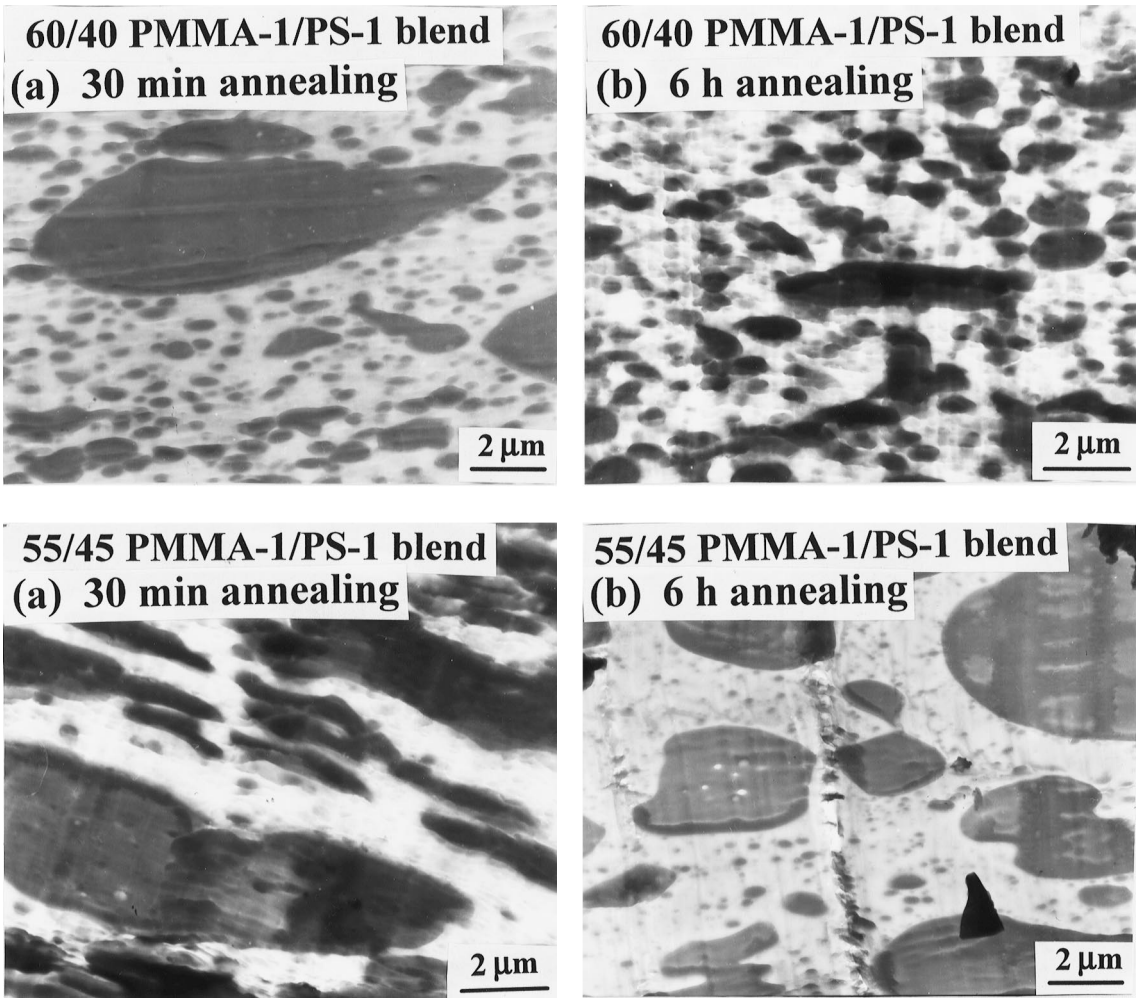

Fig. 17. The upper panel shows TEM images of a rapidly precipitated 60/40 PMMA-1/PS-1 blend after being annealed at 170°C for: (a) 30 min; (b) 6 h. The lower panel shows TEM images of a rapidly precipitated 55/45 PMMA-1/PS-1 blend after being annealed at 170°C for: (a) 30 min; (b) 6 h.

decomposition via temperature quenching. We found that the domain spacing of the modulated structure of rapidly precipitated PMMA/PS blends was the largest at an equal volume fraction and it increased with molecular weights of the constituent components. The experimental results are interpreted using the Cahn's linearized theory, which has been proven to be reasonably accurate in describing phase separation in the early stage of spinodal decomposition.

When a rapidly precipitated PMMA/PS blend was annealed under isothermal conditions at 170°C, we observed an evolution of a co-continuous morphology into a dispersed morphology, the rate of which being dependent upon the blend ratio and the molecular weights of the constituent components. We have pointed out that isothermal annealing of a rapidly precipitated PMMA/PS blend may be regarded as being equivalent to late stages of spinodal decomposition. We interpreted our experimental results of morphology evolution during isothermal annealing using Siggia's theory [33], showing that the hydrodynamic effects are very important in late stages of spinodal decomposition. We have pointed out that although, during isothermal annealing, there was no bulk flow in a rapidly precipitated blend specimen, breakup of a modulated co-continuous morphology would occur driven by the surface tension, which in turn generates a pressure gradient in the structure causing flow from a thin part to a thick part. Since the mobility of a polymer under isothermal annealing is inversely proportional to zero-shear viscosity, we have concluded that the zero-shear viscosities of the constituent polymers played an important role in controlling the growth rate, during isothermal annealing, of the discrete phase in the PMMA/PS blends investigated in the present study. Using the arguments presented above, we were able to explain our experimental results of morphology evolution, during isothermal annealing, of rapidly precipitated PMMA/PS blends.

Before closing, we would like to mention that, earlier, some research groups reported on the effect of annealing on the morphology of melt blended specimens [34–36] and, also, coalescence of the discrete phase in two-phase polymer blends [37–39]. There is no question that coalescence of the discrete phase might have taken place during the

annealing of rapidly precipitated specimens investigated in this study. Coalescence is a physical phenomenon that is associated with the kinetic process under static conditions, which inevitably would take place before reaching an equilibrium blend morphology. Coalescence of the discrete phase may also take place during the processing of a two-phase blend [36,37]. It should be mentioned that breakup of the discrete phase may also take place in pressure-driven flow of dispersed two-phase fluids [40]. To the best of our knowledge, a theoretical treatment of breakup and coalescence of the discrete phase during the processing of two-phase polymer blends has not been addressed in the literature, and requires greater attention in the future.

References

[1] Han CD, Yu TC. Polym Engng Sci 1972;12:81.
[2] Han CD, Kim YW. Trans Soc Rheol 1975;19:245.
[3] Han CD, Kim YW, Chen SJ. J Appl Polym Sci 1975;19:2831.
[4] Nelson CJ, Avgeropoulos GN, Weisser FC, Böhm GGA. Angew Makromol Chem (Vol. 60–61) 1977:49.
[5] van Oene H. In: Paul DR, Newman S, editors Polymer blends, vol 1 New York: Academic Press, 1978:295.
[6] Han CD. In: Rheology in polymer processing, chap 7 New York: Academic Press, 1976.
[7] Han CD. In: Multiphase flow in polymer processing, chap 4 New York: Academic Press, 1981.
[8] Shih C-K, Tynan DG, Denelsbeck DA. Polym Engng Sci 1991;31:1670.
[9] Lindt JT, Ghosh AK. Polym Engng Sci 1992;32:1802.
[10] Sundararaj U, Macosko CW, Rolando RJ, Chan HT. Polym Engng Sci 1992;32:1814.
[11] Shih C-K. Polym Engng Sci 1995;35:1688.
[12] Scott CE, Macosko CW. Polymer 1995;36:461.
[13] Sundararaj U, Macosko CW, Shih C-K. Polym Engng Sci 1996;36:1769.
[14] Miles IS, Zurek A. Polym Engng Sci 1988;28:796.
[15] Ho EM, Wu CH, Su AC. Polym Engng Sci 1990;30:511.
[16] Favis BD, Therrien D. Polymer 1991;32:1474.
[17] Hietaoja PT, Holsti-Miettinen RM, Seppälä JV, Ikkala OT. J Appl Polym Sci 1994;54:1613.
[18] Lehr MH. Polym Engng Sci 1985;25:1056.
[19] Yang K, Han CD. Polymer 1996;37:5795.
[20] Cahn JW. Acta Metall 1961;9:795.
[21] Cahn JW. Trans Met Soc 1968;242:166.
[22] McMaster L. Adv Chem Ser 1975;142:43.
[23] Inoue T, Ougizawa T, Yasuda O, Myasaka K. Macromolecules 1985;18:57.
[24] Snyder HL, Meakin P, Reich S. Macromolecules 1983;16:757.
[25] Strobl GR. Macromolecules 1985;18:558.
[26] Hashimoto T, Itakura M, Hasegawa H. J Chem Phys 1986;85:6118.
[27] Takenaka M, Tanaka K, Hashimoto T. In: Culbertson BM, editor Multiphase macromolecular systems New York: Plenum, 1989:363.
[28] Takenaka M, Izumitani T, Hashimoto T. J Chem Phys 1990;92:4566.
[29] Hashimoto T, Takenaka M, Izumitani T. J Chem Phys 1992;97:679.
[30] Takenaka M, Izumitani T, Hashimoto T. J Chem Phys 1992;97:6855.
[31] Nakai A, Shiwaku T, Wang W, Hasegawa H, Hashimoto T. Macromolecules 1996;29:5990.
[32] Takeno H, Hashimoto T. J Chem Phys 1997;107:1634.
[33] Siggia ED. Phys Rev A 1979;20:595.
[34] Jang B, Uhlmann D, Sande J. Rubber Chem Technol 1983;57:291.
[35] Cheng T, Keskkular H, Paul D. J Appl Polym Sci 1992;45:1245.
[36] Andradi L, Hellman G. Polym Engng Sci 1995;35:693.
[37] Fortelny I, Kovar J. Angew Makromol Chem 1988;164:125.
[38] Fortelny I, Kovar J. Eur Polym J 1988;25:317.
[39] Fortelny I, Kovar J. Polym Compos 1998;9:119.
[40] Chin H, Han CD. J Rheol 1980;24:1.